Palladated chitosan-halloysite bead as an efficient catalyst for hydrogenation of lubricants

Mona Alleshagh, Samahe Sadjadi, Hassan Arabi, Naeimeh Bahri-Laleh, Eric Monflier

Palladated chitosan-halloysite bead as an efficient catalyst for hydrogenation of lubricants

Mona alleshagh[a], Samaheh Sadjadi[b*], Hassan Arabi[a], Naeimeh Bahri-Laleh[a], Eric Monflier[c]

[a]*Polymerization Engineering Department, Iran Polymer and Petrochemical Institute (IPPI), P.O. Box 14965/115, Tehran, Iran. Tel: +982148662479, Fax: 982144787021. E-mail: n.bahri@ippi.ac.ir*

[b]*Gas Conversion Department, Faculty of Petrochemicals, Iran Polymer and Petrochemical Institute, PO Box 14975-112, Tel: +982148662478, Fax: 982144787021. Tehran, Iran. E-mail: s.sadjadi@ippi.ac.ir*

[c] *Univ. Artois, CNRS, Centrale Lille, Univ. Lille, UMR 8181, Unite de Catalyse et de Chimie du Solide (UCCS), 62300, Lens, France*

Keywords: Hydrogenation, Catalyst, Halloysite, Chitosan, Bead, Polyalphaolefins

Abstract

As hydrogenation of poly alpha-olefin (PAO) oils is an important industrial process for production of high-performance engine lubricants, in this research, a novel bio-based catalytic composite has been designed for promoting this process under relatively mild reaction condition. In this regard, chitosan and halloysite that are naturally occurring compounds with excellent performance as catalyst supports have been used for the formation of chitosan-halloysite beads. The resultant beads have been subsequently cross-linked with glutaraldehyde and palladated to furnish the final catalyst. The catalytic activity of the as-prepared catalyst was studied in the hydrogenation of PAO

obtained from oligomerization of 1-decene. In this line, the reaction variables, including, reaction temperature, hydrogen pressure and catalyst loading have also been optimized. Moreover, the effect of the content of halloysite on the performance of the catalyst has been investigated. It was found that using 5 wt.% catalyst with chitosan: halloysite mass ratio of 1:1 and hydrogen pressure of 8 bar at 130 ºC, hydrogenation proceeded to furnish the hydrogenated product in 98% yield. Notably, recyclability and hot filtration tests confirmed high recyclability of the catalyst and its heterogeneous nature.

1. Introduction

Polyalphaolefins, PAOs, are one of the most important member of synthetic oils that benefit from high viscosity index (VI, >125), low pour points and excellent oxidation stability [1]. Considering these unique features, they have been extensively applied in high-performance engine lubricants [2]. Crude PAOs that are obtained through oligomerization of olefins possess olefinic bonds in their structure that are susceptible to the oxidation at high temperature of applications [3]. As this feature can affect the performance of PAOs, their hydrogenations is highly demanding and accomplished as a synthetic step to furnish final product. Unfortunately, this process mostly requires harsh conditions in terms of hydrogen pressure and reaction temperature and precious metals as catalysts. These requirements enhance the risk and cost of PAO production. Hence, synthesis of catalysts with low loading of precious metals that can promote this reaction under mild condition is of great industrial importance.

Considering the fact that chitosan (CS) is one of the most abundant carbohydrates [4-6], it has been extensively applied as a biodegradable and biocompatible compound for various uses [7-9], including catalysis [10-12]. The distinguishable feature of CS is presence of $–NH_2$ functionalities [13-17]. This characteristic allows modification of CS properties through introduction of

functional groups [18-22] and grafting of some catalytic species, such as enzymes on it. Furthermore, other catalytic species, such as metallic nanoparticles (NPs) can be efficiently stabilized on CS through electrostatic interactions. CS can also be utilized in the formation of related beads through dropping of acidic solution of CS into an alkaline solution. The aforesaid beads can be further cross-linked to furnish more stable beads [23]. It is also possible to form composite beads by introduction of an additional component along with CS.

Halloysite, HNT, is a biocompatible clay of Kaolin group with the formula of $Al_2(OH)_4Si_2O_5.nH_2O$. The most predominant morphology of HNT is tubular morphology [24, 25], in which siloxane groups is located on the outer surface, while gibbsite octahedral sheet forms interior surface [26]. The pore space and aspect ratio of HNT are 14-46.8% and 10-50 respectively. These features as well as oppositely charged surfaces, high chemical and mechanical strength and the possibility of tuning the surface chemistry of HNT through chemical modifications rendered HNT one of the most appealing catalyst supports for designing heterogeneous catalysts [27, 28].

In the continuation of our research on developing mild methodologies for PAO hydrogenation [29-31], in this research we wish to report preparation, characterization and catalytic performance of a novel catalytic composite (Pd/CCS-HNT) based on palladated cross-linked CS-HNT beads.

2. Experiments

2.1.Materials and instruments

In this study, HNT, CS (Mw = 50000-190000, with deacetylation degree ≥ 75%, viscosity 20 cP for 1 wt.%, in 1% acetic acid), $Pd(OAc)_2$, toluene, $NaBH_4$, glutaraldehyde (GA), methanol (MeOH), tripolyphosphate (TPP) were used for the synthesis of Pd/CS-HNT beads. All the aforesaid chemicals and solvents were provided from Sigma-Aldrich, Germany. To prepare PAO, 1-decene and $AlCl_3$ were used, both were purchased from Merck Co. Germany.

The synthesized PAO was characterized via gel permeation chromatography (GPC Agilent 1100) using PS standards, kinematic viscosimetry at 40 and 100 ºC, and viscosity index (KV^{40}, KV^{100} and VI were measured according to the ASTM D445 and ASTM D 97 test methods respectively),

To characterize the as prepared Pd/CS-HNT beads, the following instruments were employed:

PERKIN ‑ ELMER ‑ Spectrum 65 spectrometer, with KBr pellets (for conducting Fourier transform infrared (FT-IR) spectroscopy), Siemens, D5000 diffract meter using Cu-Kα radiation as the X-ray source (for recording X-ray diffraction (XRD) pattern), Philips CM30300Kv instrument (for recording Transmission electron microscopy (TEM) images), Vistapro (for Inductively Coupled Plasma (ICP-AES)), VEGAII TESCAN scanning electron microscope equipped with QX2, RONTEC energy dispersive X-ray analyzer (for scanning electron microscope (SEM), Energy dispersive spectroscopy (EDS) and mapping analysis), METTLER TOLEDO thermo gravimetric analysis apparatus under N_2 atmosphere with a heating rate of 10 °C min^{-1} (for obtaining thermograms of the catalyst, HNT and CS).

The yield of hydrogenation of PAO was calculated via ^{1}HNMR spectroscopy (Bruker DRX 400 MHz NMR spectrometer) in deuterated chloroform at ambient temperature. To this purpose, the integral of the olefinic hydrogens of un-hydrogenated and hydrogenated PAO were measured and compared.

2.2.PAO synthesis

Using our previously reported procedure, PAO was prepared via oligomelization of 1-decene [32]. Briefly, monomer (500 mL) mixed with 0.3 mL deionized water (as electron donor, $H_2O/AlCl_3$ = 0.44 mol/mol) as well as $AlCl_3$ (5 g) were placed in a reactor that its air has been replaced with Ar gas and preheated to 75 °C. Then, the reaction mixture was stirred at 100 °C for 1 h. Upon

completion of oligomerization, the resulting PAO was washed with a solution of 5 wt. % NaOH several times. Finally, to remove the unreacted monomer, low molecular weight by-products and water, the product was heated under -0.8 bar vacuum up to 250 °C. Using this procedure, PAO was achieved with 86 % yield. The obtained PAO was then characterized via GPC (Figure 1) and kinematic viscosimetry. The results indicated that the as-prepared PAO possesses M_n=1710 g/mol, PDI=1.4, KV^{40}=245.5 cSt, KV^{100}=32.1 cSt and VI=132.

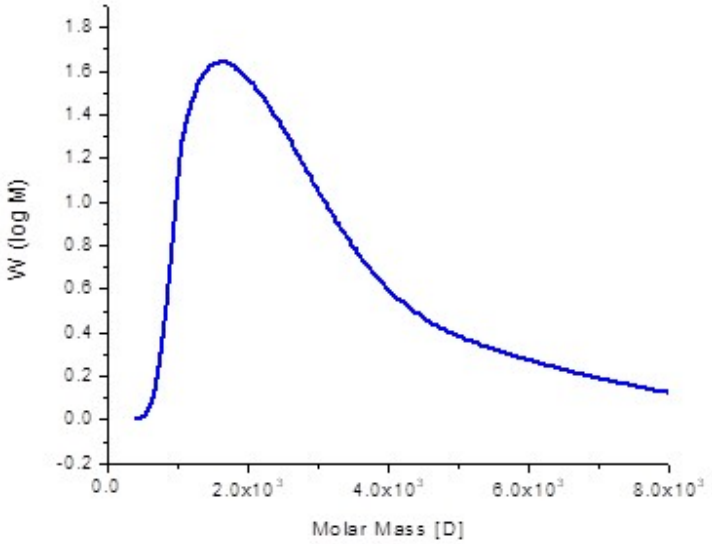

Figure 1. GPC curve of the as-synthesized PAO.

2.3.Catalyst preparation

2.3.1. Synthesis of CS-HNT beads

In this research, three CS-HNT beads with different CS: HNT mass ratios (1:1, 3:1 and 5:1) were prepared. In this regard, CS (0.5 g), was dissolved in acetic acid solution (2 wt.%, 50 mL) and then, appropriate amount of HNT was introduced to the aforementioned solution. The resultant suspension, denoted as suspension A, was stirred at room temperature for half an hour. Meanwhile, a basic solution, denoted as solution B, was prepared by dissolving TPP (1 g) in distilled water (100 mL). Subsequently, suspension A was transferred into a burette and slowly dropped into the

solution B to form tiny beads. The as-prepared beads were kept in solution B for 7 h and then, washed with distilled water repeatedly to reach pH = 7. The yield of the reaction is 80%.

2.3.2. Cross-linking of CS-HNT beads: CCS-HNT

The as-prepared wet beads were suspended in GA solution in EtOH (5 wt.%) and stirred for 24 h at 70 ºC. Upon completion of the reaction, the cross-linked beads (CCS-HNT), with yield of 90 %, were washed with EtOH and dried at ambient temperature overnight, Figure S1. According to the TG analysis, the degree of cross-linking was 20%.

2.3.3. Stabilization of Pd NPs

A solution of $Pd(OAc)_2$ in toluene (0.02 g in 15 mL), was prepared and gently dropped in the stirring suspension of cross-linked CS-HNT beads. Afterwards, the obtained mixture was stirred for 2 h at ambient temperature. Then, fresh solution of $NaBH_4$ (0.12 g in 15 mL MeOH) was prepared and slowly added to the aforementioned mixture under inert atmosphere. After stirring for 3 h, the palladated beads were separated, washed with MeOH and dried at room temperature, Figure 2. ICP analysis established that Pd content in Pd/CCS-HNT was 0.6 wt.%.

2.4.Hydrogenation of PAO

To examine the efficiency of the as-prepared Pd/CCS-HNT for hydrogenation of PAO, a stainless steel reactor was charged with PAO (10 g) and appropriate amount of Pd/CCS-HNT (3-6 wt.%). The reactor was purged with dry nitrogen at 100 °C for 1 h. After that, the reactor was completely sealed and the temperature (120-140 ºC) and hydrogen pressure (5-8 bar) were adjusted. After stirring for appropriate reaction time (6 h), the reactor was cooled, discharged and subsequently the Pd/CCS-HNT catalyst was separated by decanting and the hydrogenation yield was measured via ^{1}HNMR spectroscopy.

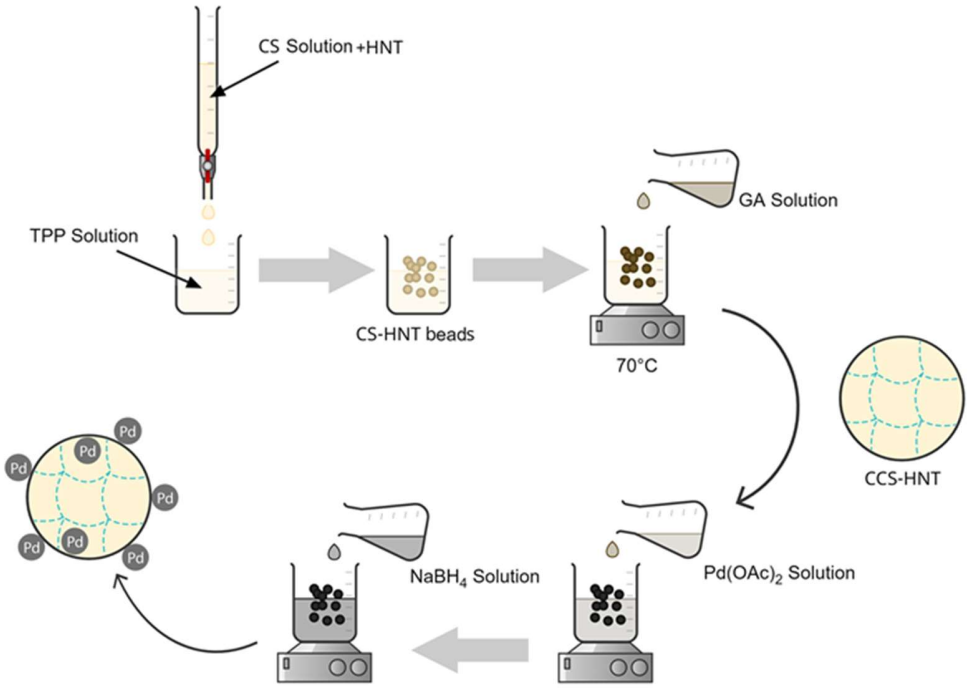

Figure 2. Schematic illustration of synthesis of Pd/CCS-HNT.

3. Result and discussion

3.1.Characterization

The SEM images of three catalysts, Pd/CCS-HNT (1:1), Pd/CCS-HNT (3:1) and Pd/CCS-HNT (5:1), are depicted in Figure 3. As shown, the content of HNT can affect the morphology of the resultant catalysts and Pd/CCS-HNT (1:1) that contains the highest content of HNT showed smoother surface, while, Pd/CCS-HNT (3:1) and Pd/CCS-HNT (5:1) exhibited rough and porous surface. The diameters of Pd/CCS-HNT (1:1), Pd/CCS-HNT (3:1) and Pd/CCS-HNT (5:1) beads were 1.35, 1.15 and 1.23 mm respectively.

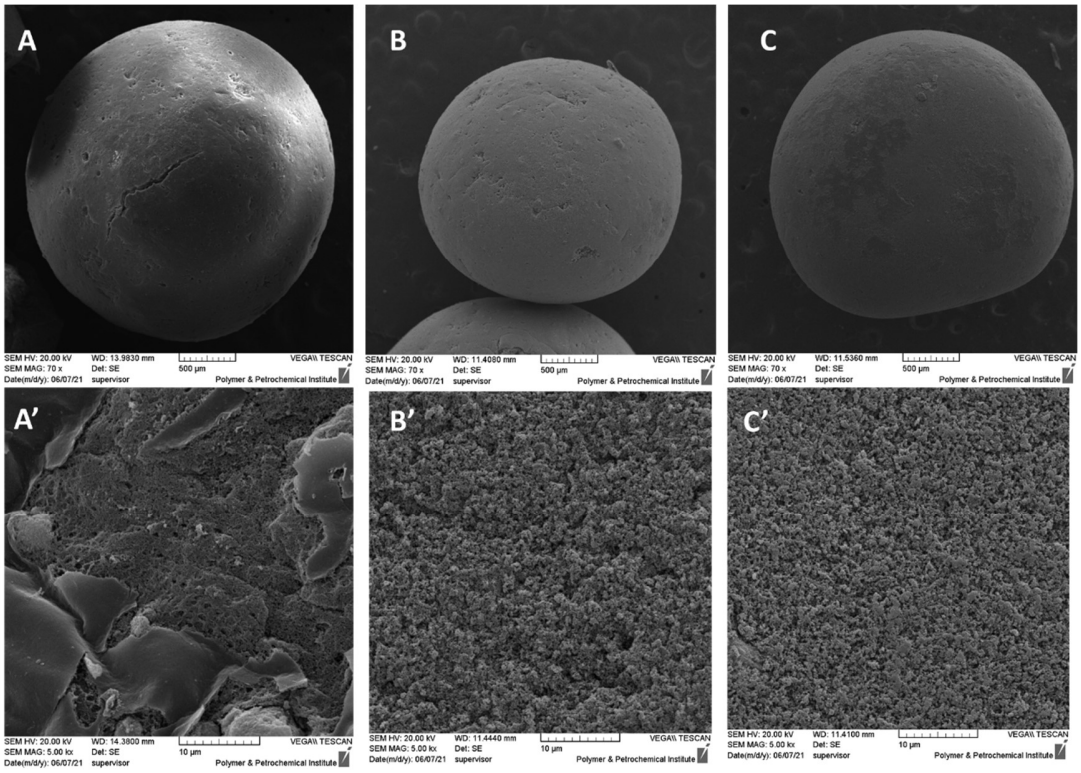

Figure 3. SEM images of palladated chitosan-halloysite beads at different magnifications (x 70 and x 5000) : Pd/CCS-HNT (1:1) (A and A'), Pd/CCS-HNT (3:1) (B and B') and Pd/CCS-HNT (5:1) (C and C').

One of the TEM image of Pd/CCS-HNT (1:1), as well as the particle size distribution curve of Pd NPs are shown in Figure 4. As depicted, HNT tubes are observable in the TEM image of Pd/CCS-HNT, confirming that HNT tubular morphology remained intact in the course of formation of beads. Furthermore, it can be discerned that HNT tube is covered with CS (the fine sheet-like part in the TEM picture). Moreover, Pd NPs with average particle size of 2.13±0.02 have been well-dispersed on the CCS-HNT and no aggregation was observed.

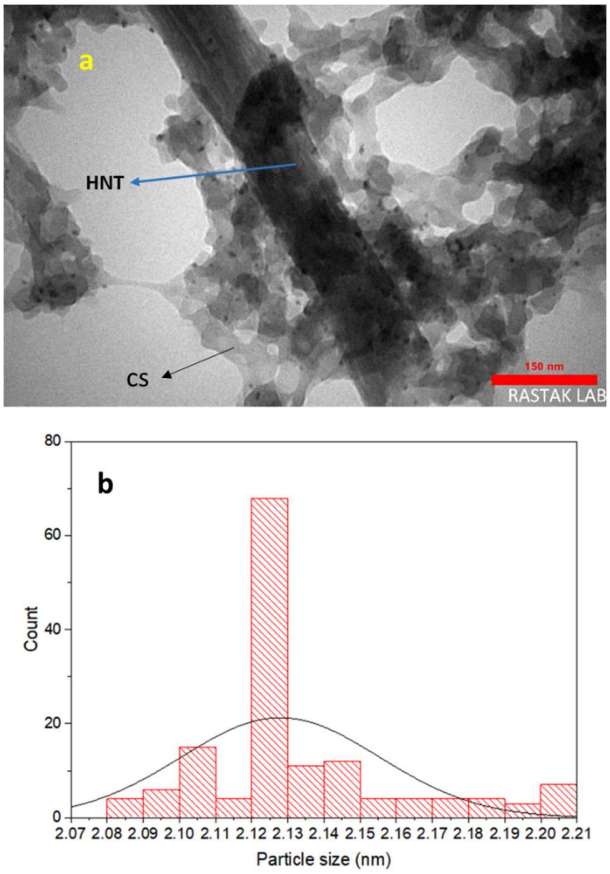

Figure 4. a) TEM image of the catalyst and b) particle size distribution curve of Pd NPs.

Characterization of Pd/CCS-HNT(1:1) via EDS analysis, Figure 5, indicated the presence of C, O, N, Si, Al, Pd atoms in the structure of the as-prepared beads. Among the detected atoms, C, O and N can be assigned to CCS, while Si, Al and O are indicative of HNT. Observation of Pd atoms in EDS analysis can imply the successful stabilization of Pd species on the CCS-HNT beads. The elemental mapping analysis, Figure 5, also showed high dispersion of Pd NPs. This result is in good accordance with the results of TEM.

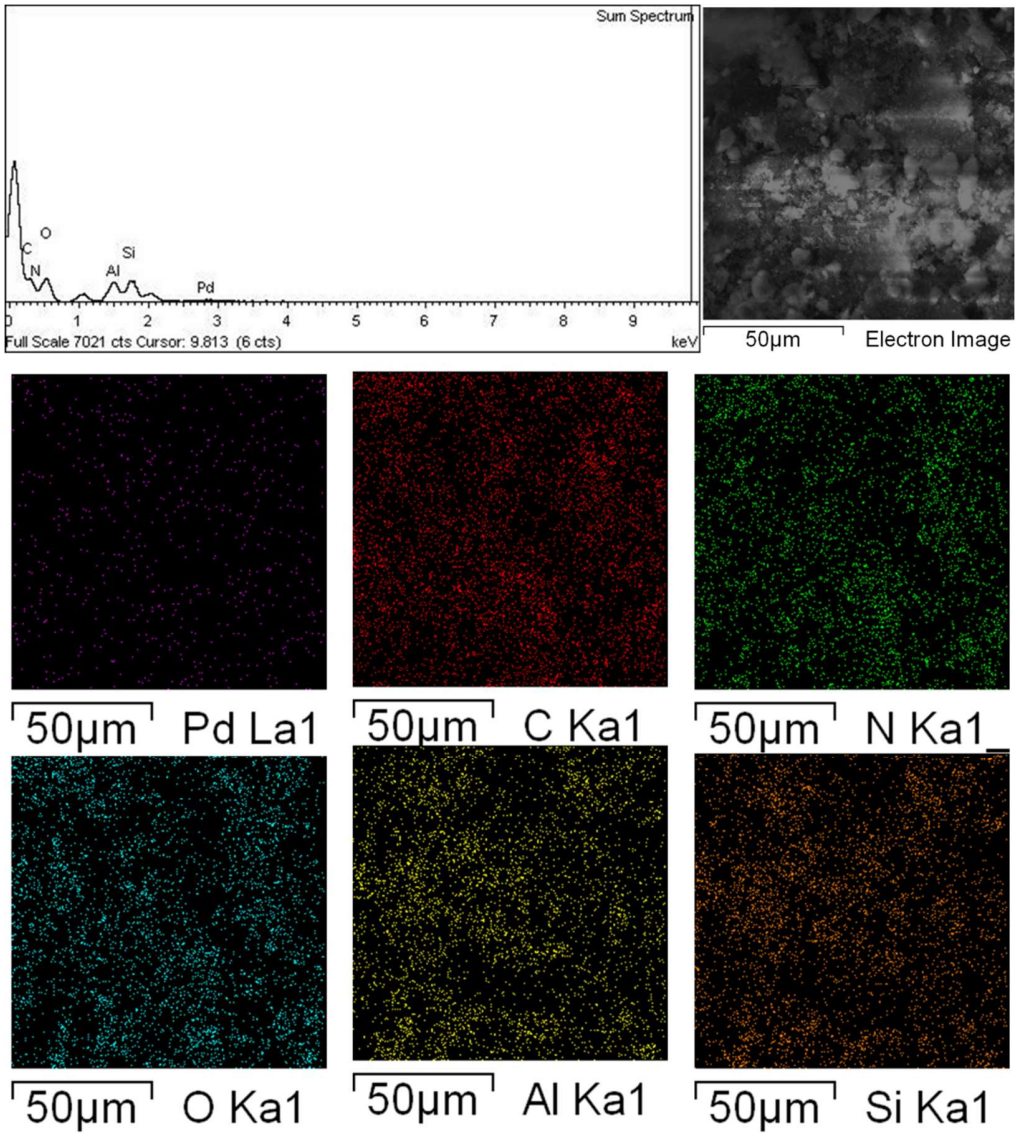

Figure 5. EDS and elemental mapping analyses of the catalyst, Pd/CCS-HNT(1:1).

To study the structure of Pd/CCS-HNT, its XRD pattern was recorded and compared with that of CS and pristine HNT. As shown in Figure 6, in the XRD pattern of CS, a broad band, spread at 2θ = 12-25º can be observed that is representative of amorphous CS [33]. In the case of HNT, the characteristic bands appeared at 2θ = 12.3°, 18.8°, 20.6°, 25.2°, 36.7°, 39.0°, 56.3° and 62.5° (JCPDS No. 29-1487) [27]. In the case of Pd/CCS-HNT, the recorded XRD pattern showed a broad band that can be attributed to amorphous CS. However, it can also be observed that some of the

characteristic bands of HNT with very low intensities are present in the XRD pattern of the catalyst. This issue has been previously reported in HNT-based composites [27]. It is worth to mention that the characteristic bands of Pd NPs that are bands with relatively low intensities were not recognizable in the XRD pattern of the catalyst. This issue can also be attributed to the formation of very fine particles with homogeneous dispersion [34].

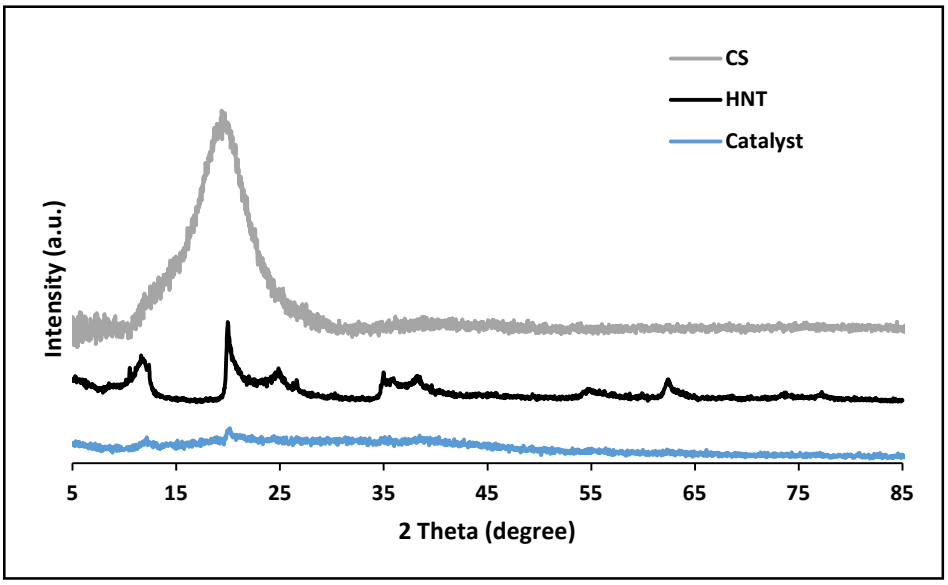

Figure 6. XRD patterns of HNT, CS and the as-prepared catalyst, Pd/CCS-HNT(1:1).

To further characterize Pd/CCS-HNT, FTIR spectrum of the as-prepared catalyst was recorded and compared with that of CS and HNT. As shown in Figure 7, the absorbance bands of CS can be observed at 3453 cm^{-1} (-OH), 2884 cm^{-1} ($-CH_2$), 16375 cm^{-1} (N–H bending vibration and stretching for primary amine) and 1051 cm^{-1} (stretching of C–O group). The absorbance bands of HNT appeared at 3697 cm^{-1} and 3626 cm^{-1} (inner -OH), 1035 cm^{-1} (Si-O stretching), 536 cm^{-1} (Al-O-Si vibration) and 1650 cm^{-1}. In the FTIR spectrum of Pd/CCS-HNT, both characteristic bands

of HNT and CS can be detected. Notably, the characteristic bands of imine functionality, formed through cross-linking of CS-HNT beads, overlapped with the characteristic bands of HNT and CS.

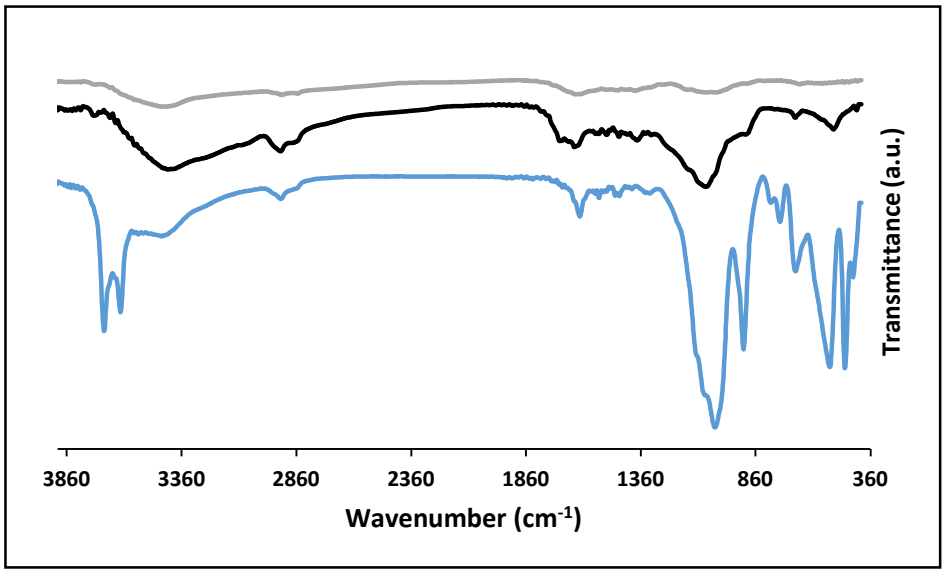

Figure 7. FTIR spectra of CS (gray), HNT (black) and the catalyst, Pd/CCS-HNT(1:1) (blue).

Next, TG analysis has been exploited to disclose the thermal stability of Pd/CCS-HNT. Furthermore, the TG curve of the bead component, i.e. HNT and CS were also recorded and compared with that of Pd/CCS-HNT, Figure 8. According to the previous reports, HNT weight losses (at 150 and 410 ºC) are due to the dehydration and dehydroxylation, respectively [27]. In the case of CS, loss of water and degradation occurred at 110 and 250 °C, respectively. In Pd/CCS-HNT TG curve, three weight losses can be detected. The first one (at 110 °C) can be assigned to the loss of water, the second one (at range of 240 -290 °C) can be attributed to the degradation of cross-linked CS component. Compared to CS, this weight loss step takes place over a wider and higher temperature range. This issue can be attributed to the cross-linked nature of CCS. The third weight loss (at 410 °C) can be assigned to the dehydroxylation of HNT in the structure of the bead.

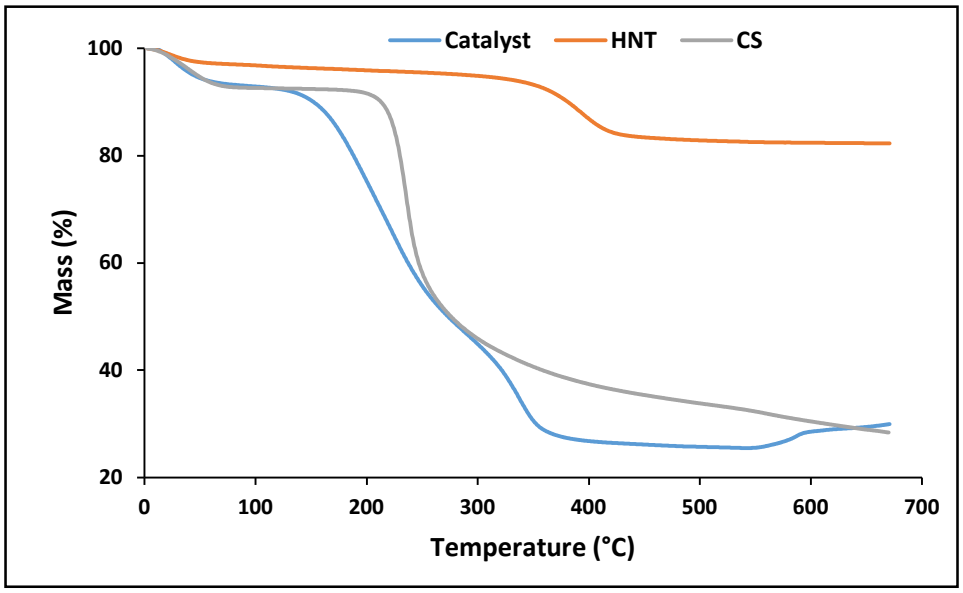

Figure 8. TG curves of CS, HNT and Pd/CS-HNT(1:1).

3.2.PAO hydrogenation

The influential parameters on the hydrogenation yield of PAO are reaction temperature, hydrogen pressure and Pd/CCS-HNT(1:1) dosage. Hence, to achieve the highest reaction yield, optimization of these parameters is imperative. On the other hand, it was assumed that the nature of the CS-HNT beads can affect the activity of the resultant catalyst. Therefore, the effect of the content of HNT in CS-HNT bead was also investigated (vide infra).

3.3.The effect of reaction temperature

To optimize the reaction temperature, PAO hydrogenation was accomplished under hydrogen pressure of 8 bar at three different temperatures (120, 130 and 140 ºC). The results inferred that by increasing temperature from 120 to 130 ºC, the hydrogenation yield improved, while further increase of this value to 140 ºC had no significant effect, Table 1. Hence, 130 ºC was chosen for further experiments.

3.4.The effect of catalyst dosage

To study the effect of Pd/CCS-HNT (1:1) loading on the yield of PAO hydrogenation and optimize this parameter, hydrogenation of PAO at 130 ºC and hydrogen pressure of 8 bar was done by using different Pd/CCS-HNT dosage (3-6 wt.%). Comparison of the reaction after 6 h indicated that catalyst content significantly affected the yield of hydrogenation reaction and use of 5 wt.% catalyst led to the hydrogenated PAO in highest yield (98%), Table 1. Noteworthy, increase of Pd/CCS-HNT loading to 6 wt.% was not efficient.

3.5.The effect of hydrogen pressure

Hydrogen pressure is one of the most important parameters in hydrogenation reactions. Low hydrogen pressure can assure the safety and economy of the process. To achieve the optimum value of this parameter, PAO hydrogenation was performed in the presence of 5 wt.% Pd/CCS-HNT (1:1) at 130 ºC under three different pressures, 5, 7 and 8 bar. The results showed that moderate yields were achieved at low hydrogen pressure and increase of this parameter effectively increased the reaction yield and accelerate the reaction rate, Table 1. More precisely, ^{1}HNMR spectroscopy, Figure S2, showed that using hydrogen pressure of 8 bar under the aforementioned condition, hydrogenated PAO with 98% yield was achieved after 6 h (Figure S2).

Table 1. Optimization of reaction variable for PAO hydrogenation using Pd/CCS-HNT (1:1) catalyst.

Entry	Pd/CCS-HNT (1:1) (w/w %)	Temp. (°C)	Time (h)	Pressure (bar)	Yield (%)
1	**5**	**130**	**6**	**8**	**98**
2	5	130	7	7	80
3	5	130	9	5	65
4	6	130	6	8	98
5	3	130	9	8	60
6	5	120	6	8	87
7	5	140	6	8	98

PAO amount: 10 g

3.6.The effect of HNT content

It was postulated that the mass ratio of CS: HNT may affect the performance of the resulting catalyst. To elucidate the effect of this parameter, three CS-HNT beads with CS: HNT mass ratios of 1:1, 3:1 and 5:1 were prepared, cross-linked, palladated and then applied for PAO hydrogenation. As expected, the activities of three catalysts were distinguishable and the yield of hydrogenation of these three catalysts followed the order of Pd/CCS-HNT (1:1) (98%)> Pd/CCS-HNT (5:1) (73%)> Pd/CCS-HNT (3:1) (65%). In fact, the catalyst with the highest content of HNT, Pd/CCS-HNT (1:1), exhibited the highest catalytic activity and the activity of Pd/CCS-HNT (5:1) was slightly higher than that of Pd/CCS-HNT (3:1).

To find out the origin of the difference of the catalytic activity of these catalysts, they have been characterized. As discussed above, SEM analysis, Figure 3, indicated that the morphology of

Pd/CCS-HNT (1:1) sample, is different and distinguished from Pd/CCS-HNT (5:1) and Pd/CCS-HNT (3:1).

ICP results also confirmed that HNT content could affect the loading of Pd NPs. More precisely, the content of Pd NPs in the three samples followed the order of Pd/CCS-HNT (5:1) (0.86 wt%)> Pd/CCS-HNT (1:1) (0.60 wt%)> Pd/CCS-HNT (3:1) (0.48 wt%). On the other hand, measurement of Pd NPs average size in the three samples, indicated that in the samples with higher CS content, the possibility of aggregation of Pd NPs is higher and larger Pd NPs have been formed (this value for Pd/CCS-HNT (3:1) and Pd/CCS-HNT (5:1) are 2.6±0.07 and 3.0±0.05 nm respectively). Considering all of these results, it can be concluded that the content of HNT in the bead can affect the features of the catalyst in terms of Pd loading, morphology and Pd NPs average particle size and Pd/CCS-HNT (1:1), in which Pd loading is 0.60 wt% and Pd NPs average size is 2.1±0.02 nm showed the highest catalytic activity.

3.7.Hot filtration

To verify heterogeneous nature of Pd/CCS-HNT (1:1), hot filtration test was carried out. In more detail, the hydrogenation reaction under the optimum reaction was halted after 3 h and then, Pd/CCS-HNT was removed from the reactor. ^{1}HNMR spectroscopy confirmed that after 3 h, the yield of hydrogenation reaction was 40 %. Afterwards, the hydrogenation reaction was pursued in the absence of Pd/CCS-HNT and the yield of hydrogenation reaction was monitored via ^{1}HNMR spectroscopy. In the case of true heterogeneous catalysis, Pd NPs are stabilized on the support in the course of the reaction and do not leach in the reaction media. Hence, it is expected that the reaction does not proceed after catalyst removal. The results of ^{1}HNMR spectroscopy confirmed this assumption and approved heterogeneous nature of the catalysis.

3.8.Catalyst recycling

As low leaching of catalytic species, stability of the catalyst and preserving catalytic performance are important factors for large scale applications, recyclability of Pd/CCS-HNT (1:1) for PAO hydrogenation under optimized condition was examined. For the recovery of the catalyst, it was washed with hexane repeatedly and then dried in oven at 60 ºC. The recovered Pd/CCS-HNT was then applied for the next run of PAO hydrogenation. The recovery-reuse cycle was repeated for four consecutive runs and the yield of hydrogenated PAO after each run was estimated and compared with that of fresh Pd/CCS-HNT. As summarized in Figure 9, the catalyst preserved its activity and loss of the activity after each run was negligible. The content of Pd leaching was also measured via ICP analysis and it was disclosed that Pd leaching was insignificant (1.3 wt.% of initial dosage).

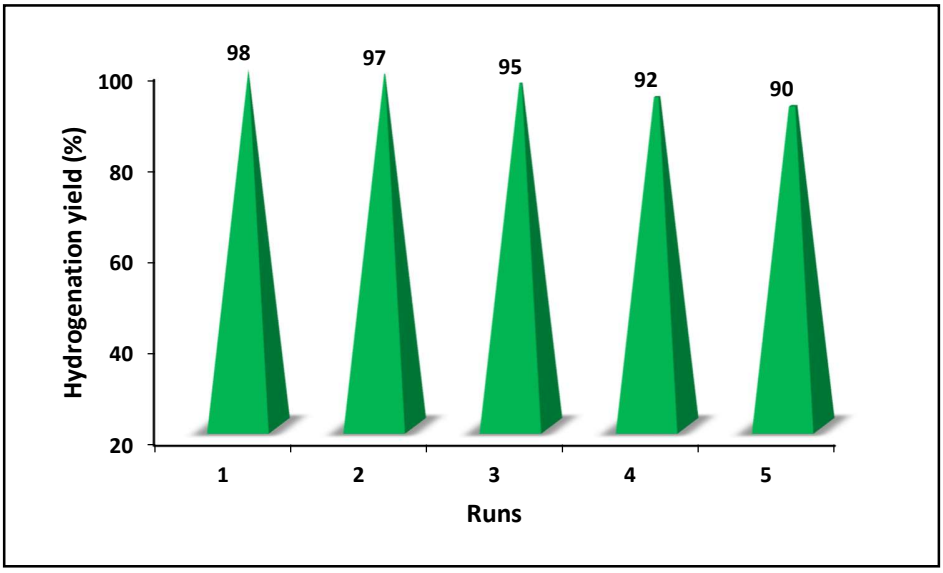

Figure 9. Yields of hydrogenated PAO after five reaction runs, using Pd/CCS-HNT (1:1) catalyst at H_2 pressure of 8 bar and T=130 ºC.

3.9.Comparative study

To the best of our knowledge, there are only three reports on the catalytic hydrogenation of PAO, all reported by our research group [29-31]. In all of the reported methodologies, HNT-based catalysts, including ligand-decorated HNT, ionic liquid-functionalized HNT and nitrogen rich polymer-HNT nanocomposite, have been utilized for the hydrogenation of PAO (derived from 1-decene). In Table 2, the hydrogenation reaction conditions, hydrogenation yields, recyclability and Pd contents of those catalysts are compared with those of Pd/CCS-HNT (1:1). The results approved that although the Pd content of Pd/CCS-HNT (1:1) is significantly lower that other three catalysts, its catalytic activity is comparable with the other catalysts. In more details, 4-5 wt. % of the mentioned catalysts could promote the hydrogenation of PAO in almost quantitative yield after 6 h at reaction temperature of 130-140 ºC. However, the hydrogen pressure required for Pd/CCS-HNT (1:1) was slightly higher than other catalysts. Furthermore, the recyclability of the tabulated catalysts are comparable. Noteworthy, the main merit of Pd/CCS-HNT (1:1) is its simplicity and low cost. More precisely, synthesis of the previously reported catalysts, Pd@HNT-IL, Pd@Hal-TCT-DA and Pd@Hal-L1A9 needed several-step procedures, while synthesis of Pd/CCS-HNT (1:1) is relatively simple and use low-cost and available raw materials. On the other hand, low content of Pd in Pd/CCS-HNT (1:1) renders this catalyst cost-effective. Moreover, the recovery of Pd/CCS-HNT (1:1) from the reaction media is more facile than other catalysts.

Table 2. Comparison of the catalytic activity of Pd/CCS-HNT (1:1) for hydrogenation of PAO (derived from 1-decene) with reported catalysts.

Entry	Catalyst	Catalyst amount (w/w %)	Temp. (°C)	Time (h)	Pressure (bar)	Yield (%)	Pd content (w/w %)	Recyclability (runs)	Ref.
1	Pd/CCS-HNT (1:1)	5	130	6	8	98	0.6	4	This work
2	Pd@HNT-IL[1]	4	130	6	6	100	2	5	[29]
3	Pd@Hal-TCT-DA[2]	4	140	6	6	99	2	5	[35]
4	Pd@Hal-L1A9[3]	5	130	6	6	98	2	4	[31]

1: HNT decorated with ionic liquid

2: nitrogen rich polymer–HNT nanocomposite

3: Ligand decorated HNT

Conclusion

Cross-linked CS-HNT beads have been synthesized through dropping acidic mixture of CS and HNT with mass ratio of 1:1 to TPP solution, followed by cross-linking with GA. The resultant beads were then palladated through wet-impregnation method and applied for hydrogenation of PAO lubricants. The reaction variables, including, catalyst dosage, reaction temperature and hydrogen pressure were optimized. Under the optimum hydrogenation condition, i.e. hydrogen pressure of 8 bar, reaction temperature of 130 ºC and catalyst loading of 5 wt.%, PAO has been successfully hydrogenated to furnish the hydrogenated product in 98% yield after 6 h. The effect of content of HNT in the structure of bead on the performance of the final catalyst was also studied

by preparing two other sample catalysts with CS:HNT mass ratio of 3:1 and 5:1. It was confirmed that the content of HNT can affect the morphology and Pd loading of the catalyst and the catalyst with CS:HNT mass ratio of 1:1 showed the best catalytic activity.

Acknowledgment

The authors appreciate partial support of Iran Polymer and Petrochemical Institute. Samahe Sadjadi is thankful to Iran National Science Foundation for the Individual given grant, NO. 99011126.

References

1. Zhang, Q., et al., *Preparation, characterization and tribological properties of polyalphaolefin with magnetic reduced graphene oxide/Fe3O4.* Tribol. Int., 2020. **141**: p. 105952.
2. Hanifpour, A., et al., *Coordinative chain transfer polymerization of 1-decene in the presence of a Ti-based diamine bis(phenolate) catalyst: a sustainable approach to produce low viscosity PAOs.* Green Chem., 2020. **22**(14): p. 4617-4626.
3. Hanifpour, A., et al., *Kinetic and microstructural studies of Cp2ZrCl2 and Cp2HfCl2-catalyzed oligomerization of higher α-olefins in mPAO oil base stocks production.* Polyolefins J., 2021. **8**(1): p. 31-40.
4. Franconetti, A., et al., *Native and modified chitosan-based hydrogels as green heterogeneous organocatalysts for imine-mediated Knoevenagel condensation.* Appl. Catal. A-Gen., 2016. **517**: p. 176-186.
5. Leonhardt, S.E.S., et al., *Chitosan as a support for heterogeneous Pd catalysts in liquid phase catalysis.* Appl. Catal. A-Gen., 2010. **379**(1): p. 30-37.
6. Zhao, H., J. Xu, and T. Wang, *Silica/chitosan core–shell hybrid-microsphere-supported CuI catalyst for terminal alkyne homocoupling reaction.* Appl. Catal. A-Gen., 2015. **502**: p. 188-194.
7. Torkaman, S., et al., *Modification of chitosan using amino acids for wound healing purposes: A review.* Carbohydr. Polym., 2021. **258**: p. 117675.
8. Araujo, V.H.S., et al., *Chitosan-based systems aimed at local application for vaginal infections.* Carbohydr. Polym., 2021. **261**: p. 117919.
9. Cavallaro, G., et al., *Chitosan-based smart hybrid materials: a physico-chemical perspective.* J. Mater. Chem. B, 2021. **9**(3): p. 594-611.
10. Anbu, N., et al., *Chitosan as a biodegradable heterogeneous catalyst for Knoevenagel condensation between benzaldehydes and cyanoacetamide.* Catal. Commun., 2020. **138**: p. 105954.
11. Koohestani, F. and S. Sadjadi, *Polyionic liquid decorated chitosan beads as versatile metal-free catalysts for catalyzing chemical reactions in aqueous media.* J. Mol. Liqu., 2021: p. 115754.
12. Macquarrie, D.J. and J.J.E. Hardy, *Applications of Functionalized Chitosan in Catalysis.* Ind. Eng. Chem. Res., 2005. **44**(23): p. 8499-8520.

13. Guibal, E., *Heterogeneous catalysis on chitosan-based materials: a review.* Prog. Polym. Sci., 2005. **30**(1): p. 71-109.
14. Bodhak, C., A. Kundu, and A. Pramanik, *An efficient and recyclable chitosan supported copper (II) heterogeneous catalyst for C–N cross coupling between aryl halides and aliphatic diamines.* Tetrahedron Lett., 2015. **56**(2): p. 419-424.
15. Shen, C., et al., *A highly active and easily recoverable chitosan@ copper catalyst for the C–S coupling and its application in the synthesis of zolimidine.* Green Chem., 2014. **16**(6): p. 3007-3012.
16. Sadjadi, S., M.M. Heravi, and S.S. Kazemi, *Ionic liquid decorated chitosan hybridized with clay: A novel support for immobilizing Pd nanoparticles.* Carbohydr. Polym., 2018. **200**: p. 183-190.
17. Wu, D., et al., *EDTA modified β-cyclodextrin/chitosan for rapid removal of Pb (II) and acid red from aqueous solution.* J. Colloid Interface Sci., 2018. **523**: p. 56-64.
18. Zeng, M., et al., *N-doped mesoporous carbons supported palladium catalysts prepared from chitosan/silica/palladium gel beads.* Int. J. Biol. Macromol. , 2016. **89**: p. 449-455.
19. Zeng, M., et al., *Novel macroporous palladium cation crosslinked chitosan membranes for heterogeneous catalysis application.* Int. J. Biol. Macromol. , 2014. **68**: p. 189-197.
20. Dhanavel, S., et al., *Preparation and characterization of cross-linked chitosan/palladium nanocomposites for catalytic and antibacterial activity.* J. Mol. Liq., 2018.
21. Xie, H., et al., *A chitosan modified Pt/SiO2 catalyst for the synthesis of 3-poly (ethylene glycol) propyl ether-heptamethyltrisiloxane applied as agricultural synergistic agent.* Catal. Commun., 2018. **104**: p. 118-122.
22. Akpomie, K.G., F.A. Dawodu, and K.O. Adebowale, *Mechanism on the sorption of heavy metals from binary-solution by a low cost montmorillonite and its desorption potential.* Alexandria Eng. J., 2015. **54**(3): p. 757-767.
23. Sargin, I., *Efficiency of Ag(0)@chitosan gel beads in catalytic reduction of nitroaromatic compounds by sodium borohydride.* Int. J. Biol. Macromol., 2019. **137**: p. 576-582.
24. Sadjadi, S., et al., *Eggplant-Derived Biochar-Halloysite Nanocomposite as Supports of Pd Nanoparticles for the Catalytic Hydrogenation of Nitroarenes in the Presence of Cyclodextrin.* ACS Sustain. Chem. Eng., 2019. **7**(7): p. 6720-6731.
25. Sadjadi, S., et al., *Pd nanoparticles immobilized on halloysite decorated with a cyclodextrin modified melamine-based polymer: a promising heterogeneous catalyst for hydrogenation of nitroarenes.* New J. Chem., 2018. **42**(19): p. 15733-15742.
26. Yuan, P., D. Tan, and F. Annabi-Bergaya, *Properties and applications of halloysite nanotubes: recent research advances and future prospects.* Appl. Clay Sci., 2015. **112-113**: p. 75-93.
27. Sadjadi, S., *Halloysite-based hybrids/composites in catalysis.* Appl. Clay Sci., 2020. **189**: p. 105537.
28. Massaro, M., et al., *Halloysite nanotubes as support for metal-based catalysts.* J. Mater. Chem. A, 2017. **5**(26): p. 13276-13293.
29. Sadjadi, S., et al., *Combined experimental and computational study on the role of ionic liquid containing ligand in the catalytic performance of halloysite-based hydrogenation catalyst.* J. Mol. Liq., 2021. **331**: p. 115740.
30. Karimi, S., et al., *Pd on nitrogen rich polymer–halloysite nanocomposite as an environmentally benign and sustainable catalyst for hydrogenation of polyalfaolefin based lubricants.* J. Ind. Eng. Chem., 2021.
31. Tabrizi, M., et al., *Efficient hydro-finishing of polyalfaolefin based lubricants under mild reaction condition using Pd on ligands decorated halloysite.* J. Colloid Interface Sci., 2021. **581**: p. 939-953.

32. Sadjadi, S., et al., *Rationalizing chain microstructure in the polyα-olefins synthesized by cationic $AlCl_3/H_2O$ catalytic system.* Int. J. Polym. Anal. Character., 2019. **24**(6): p. 556-570.
33. Chagas, P.M.B., et al., *Use of an environmental pollutant from Hexavalent chromium Removal as a Green catalyst in the fenton process.* Sci. Rep., 2019. **9**(1): p. 1-15.
34. Mallik, S., et al., *Synthesis, characterization, and catalytic activity of phosphomolybdic acid supported on hydrous zirconia.* J. Colloid Interface Sci., 2006. **300**: p. 237–243.
35. Karimi, S., et al., *Pd on nitrogen rich polymer–halloysite nanocomposite as an environmentally benign and sustainable catalyst for hydrogenation of polyalfaolefin based lubricants.* J. Ind. Eng. Chem . 2021. **97**: p. 441-451.